

Electroconductive Composites Containing Nanocellulose, Nanopolypyrrole, and Silver Nanoparticles

Samir Kamel^{1,*}, Ahmed A. Haroun², Amany M. El-Nahrawy³ and Mohamed A. Diab¹

¹Cellulose and Paper Department, National Research Centre, 33 El Bohouth st. Dokki Giza, P.O. 12622, Egypt.

²Industrial Research Division, National Research Centre, 33 El Bohouth st. Dokki Giza, P.O. 12622, Egypt.

³Solid State physics Department, Physics Research Division, National Research Centre, 33 El Bohouth st. Dokki Giza, P.O. 12622, Egypt.

*Corresponding Author: Samir Kamel. Email: samirki@yahoo.com.

Abstract: In this work, conducting composites of nanocellulose (NC)/polypyrrole nanoparticles (NPPy) and silver nanoparticles (AgNPs), i.e., NC/NPPyAg, were synthesized for the first time, to the best of our knowledge, via *in situ* emulsion polymerization of pyrrole in the presence of surfactant dopants. The AgNPs acted as an oxidizing agent to simultaneously incorporate nanoparticles into the prepared composites. The structures and morphologies of the prepared composites were studied using Fourier transform infrared (FTIR) spectroscopy, X-ray diffraction (XRD), UV-Vis Spectra, thermogravimetric analysis (TGA), and scanning and transmission electron microscopy (SEM and TEM) techniques. Additionally, the prepared composites were characterized by their conductivities, and the dielectric constants (ϵ'), dielectric losses (ϵ''), and AC conductivities were studied for the prepared composites with an increasing NPPy content as a function of the frequency.

Keywords: Nanocellulose; nanopolypyrrole; emulsion polymerization; silver nanoparticles; conductive nanocomposites

1 Introduction

Conducting polymers are a unique group of polymers due to their stability, facile synthesis, and simple doping/dedoping chemistry. These properties allow conducting polymers to be used in a wide variety of applications, such as rechargeable batteries, biological activity, drug release systems, and sensors. In general, conductive polymers exhibit poor electrical conductivity ($\sigma \leq 10$ - 12 S/cm) in their undoped states. To enhance their conductivities into the metallic region, these undoped polymers must be treated with a suitable oxidizing or reducing agent (doping agent) [1].

Among the numerous conducting polymers prepared to date, polypyrrole (PPy) is a promising conducting polymer for different applications, such as electronics, biological and medical areas, due to its straightforward polymerization, biocompatibility, environmental stability, and electrical conductivity, which can be controlled by changing the doping level [2]. Additionally, PPy can be synthesized by chemical and electrochemical polymerization in aqueous solutions at neutral pH [3-4]. However, the commercial applications of PPy are limited due to its poor processability and weakened mechanical properties. To overcome these problems, several methods have been studied, such as the deposition of conducting polymers on the surface of fiber fabrics through the *in situ* oxidative polymerization of pyrrole (Py) [5-6]. Optimized conditions for the oxidation of Py with ferric chloride [7-8], ammonium peroxydisulfate, or ceric sulfate [9] have been extensively reported in the literature. Additionally, over the past few years, the deposition of PPy on the surface of fabrics through the *in situ* oxidative polymerization of Py using oxidizing agents, such as ferric chloride [10] or ammonium persulfate [11], has been widely

investigated. For example, highly flexible paper-like materials of PPy/tunicate cellulose nanocrystal nanocomposites using ammonium persulfate as an oxidant have been proposed as sensors, electronic devices, antistatic and anticorrosive nanocoatings, intelligent clothes, flexible electrodes, and tissue engineering scaffolds [12]. Kim [13] prepared cellulose filter paper coated by PPy using FeCl_3 as an oxidant and doped with anthraquinone-2,6-disulfonic acid via electropolymerization. The authors found that the charge-storage capacity was dependent on the amount of electropolymerized PPy.

According to literature surveys, composite materials featuring conducting polymers with noble metals have gained increasing attention only during the past few years. These composites [11] have beneficial properties, such as ionic properties, optical activity, and flexibility, in addition to the usual properties of the conducting polymers; the additional properties allowed these composites to be used in many applications [14]. Silver is one such metal that has been used in these composites; silver exhibits the highest electrical conductivity among all other metals, is relatively cheap compared to other noble metals and can be incorporated as microspheres, microparticles, nanofibers, nanorods, or nanowires [15].

The available strategies for preparing of PPy/Ag composites are: (i) dispersion of silver nanoparticles (AgNPs) on the polymer surface or in a polymer matrix; (ii) *in situ* polymerization of PPy around AgNPs [16]; (iii) reduction of silver ions using the polymer or monomer as a reducing agent [17]. The use of AgNO_3 as an oxidizing agent in the chemical polymerization of Py is the most efficient way to prepare conducting PPy-Ag composites.

The objective of the present work was to prepare a conducting nanocomposite from nanocellulose (NC), PPy nanoparticles (NPPy) and AgNPs. To accomplish this, NC extracted from bagasse doped PPy was prepared via the chemical oxidative polymerization of Py with NC as both a polymeric template and dopant using AgNO_3 as an oxidant in aqueous solution, and this material was simultaneously incorporated with AgNPs into prepared nanocomposites. We studied the influences of the AgNPs and Py concentrations on the electrical conductivity of the nano-cellulose (NC)/NPPy-Ag nanocomposites.

2 Materials and Experimental

2.1 Materials

Py was supplied by Sigma Aldrich Chemie GmbH. Sodium dodecylsulphate (SDS), used as a surfactant and dispersant, was purchased from Fluka BioChemika. Analytical grade silver nitrate was used in this work. Bleached Kraft pulp was kindly provided by the IDFO Company, Egypt. The ash contents of α -cellulose, lignin, hemicelluloses, and bagasse pulp were 77.60, 0.87, 21.40, and 1.30%, respectively.

2.2 Experimental

2.2.1 Preparation of Nano-Cellulose (NC)

NC was prepared from bleached bagasse pulp by acid hydrolysis, as described in the literature [18]. Briefly, the hydrolysis was performed with a H_2SO_4 solution (64% (w/w), 1:10 g/ml cellulose: dilute H_2SO_4) at 45°C for 30 minutes under vigorous and constant mechanical stirring. The hydrolysis reaction was quenched by adding excess chilled distilled water followed by successive centrifugation to remove the acidic solution. Then, the sediment was collected, resuspended in distilled water and dialyzed in a dialysis bag (400000 cut) for several days against distilled water until neutrality (pH 6-7) was reached. After this dialysis process, the sample was sonicated for 10 minutes. The produced aqueous suspension was stored in a refrigerator at 4°C until further use.

2.2.2 Preparation of NC/NPPy-AgNP Nanocomposites

The NC/NPPy-AgNP nanocomposite was prepared by the oxidation of Py with AgNO₃. The AgNO₃-to-Py molar ratio was 2.3. SDS (10% to Py) was dissolved in a minimal amount of distilled water (approximately 10 ml) until SDS completely dissolved with stirring over 30 minutes. Py was added dropwise to the SDS solution under continuous stirring, and an aqueous solution of AgNO₃ in 5 ml of distilled water was added dropwise to the mixture. The polymerization process was carried out under stirring overnight at 25°C. The black NPPy precipitate was filtered, washed with water and finally dried at 40°C overnight.

For preparation of NC/NPPyAg nanocomposites, suspended solution of NC with AgNO₃ was added to Py/SDS mixture. The relative reagents ratio used for preparing different composites are listed in Tab. 1.

Table 1: Reagents ratio for composites synthesis/2 g of NC

Pyrrole (mL)	0.0	5.0	6.7	10.0	16.7	16.7
AgNO ₃ (gm)	1.3	1.3	1.7	2.6	4.3	4.3
Sample Code	S1	S2	S3	S4	S5	S6

2.2.3 Characterization

Fourier Transform Infrared (FTIR) Spectroscopy

FTIR spectra of the NC, NPPy/AgNPs, and NC/NPPyAg nanocomposites were recorded with a FTIR spectrometer (Nicolet Impact-400 FT-IR spectrophotometer) in the wavelength range of 200-4000 cm⁻¹. The dried samples were ground into powder and then blended with KBr before pressing the mixture into ultra-thin pellets. Fine and homogeneous pellets of the different samples were back-loaded into the sample holder.

X-ray Diffraction (XRD)

The XRD patterns of the NC/NPPyAg nanocomposites were measured on a Diano X-ray diffractometer using a Cu (K α 1/K α 2) radiation source energized at 45 kV and a Philips X-ray diffractometer (PW 1930 generator, PW 1820 goniometer). The XRD patterns were recorded in a 2 θ diffraction angle range from 10° to 80°.

Transmission Electron Microscopy (TEM)

TEM (JSM 6360 LV, JEOL/Noran) was used to determine the morphologies and dimensions of the NC and NPPy. A drop of a dilute aqueous suspension was deposited on the surface of a copper grid coated with a thin carbon film. The sample was dried before TEM analysis, which was carried out with an accelerating voltage of 100-120 kV. Additionally, energy dispersive X-ray (EDX) analysis was carried out to support the presence of AgNPs in the prepared composite.

Thermogravimetric Analysis (TGA)

The thermal stabilities of the NC, NPPy/AgNPs, and NC/NPPy-AgNPs nanocomposites were tested by TGA (SDTQ 600 (USA)) at a heating rate of 10 °C/min from 25°C to 800°C under a nitrogen atmosphere.

UV-Vis-Near-IR (NIR) Spectra

A UV-Vis-NIR spectrum of the NC/NPpy-AgNPs nanocomposite was measured using a Hitachi U-2010 spectrometer.

Dielectric Measurements

The samples were pressed into tablets with thickness 1.3 mm and radius 6 mm for dielectric spectroscopy measurements. The samples tablets were put between two parallel copper electrodes connected to computerized LCR meter, 3532-50 LCR HiTester, in order to measure the dielectric spectroscopy in the frequency range of 0.1 Hz-100 KHz.

Dielectric spectroscopy was used to study the different dielectric parameters, such as the capacitance (C), dielectric constant (ϵ'), loss (ϵ''), and conductance (G), as functions of the frequency. The frequency dependences of the dielectric parameters of the polymeric material measure the responses of the material to the applied field and provide excellent information for characterizing the electrical properties. The total permittivity is given by:

$$\epsilon^* = \epsilon' - i \epsilon''.$$

The first term is the dielectric constant and measures the ability of the system to store energy and is given by $(\epsilon') = dC/\epsilon_0 A$, while the second term is the dielectric loss and measures the energy loss and is given by $(\epsilon'') = Gd/\epsilon_0 A\omega$. A is the electrode surface area, d is the sample thickness, and ω is the angular frequency [19-20].

3 Results and Discussion

3.1 FTIR Spectroscopy

The FTIR spectra of the NC, NC/AgNP, NPPy/AgNP, and NC/NPPy-AgNP nanocomposite are shown in Fig. 1. The peaks near 3400 cm^{-1} and 2920 cm^{-1} are attributed to cellulosic O-H groups and a C-H asymmetrical stretching vibration, respectively. The absorption band at 1030 cm^{-1} is attributed to the contribution of various functional groups, such as C-O and C-O-C groups (Fig. 1(a)). As shown in Fig. 1(b), the peaks at 3400 cm^{-1} , 1550 cm^{-1} , and 1450 cm^{-1} can be attributed to N-H stretching vibrations, C-N stretching vibrations, and C-C asymmetric and symmetric ring stretching vibrations, respectively. The peaks near 1175 cm^{-1} and 911 cm^{-1} indicate the doping state of NPPy, while the peak at 1035 cm^{-1} is attributed to C-H and N-H deformation vibrations. The band at 1280 cm^{-1} corresponds to the C-H and C-N in-plane deformation vibrations. These characteristic peaks of NC and NPPy were also found in the FTIR spectra of the prepared NC/NPPy-AgNPs nanocomposite (Fig. 1(c)), with the band at 1540 cm^{-1} in pure NPPy shifting to $\sim 1530 \text{ cm}^{-1}$ and the peaks corresponding to the O-H groups weakening. These peaks indicate the coating of NC by NPPy. The shifting of the band at 1540 cm^{-1} and weakening of the O-H absorption band confirmed that the O-H groups of cellulose are intermolecularly bonded to the N-H groups in the Py ring [21].

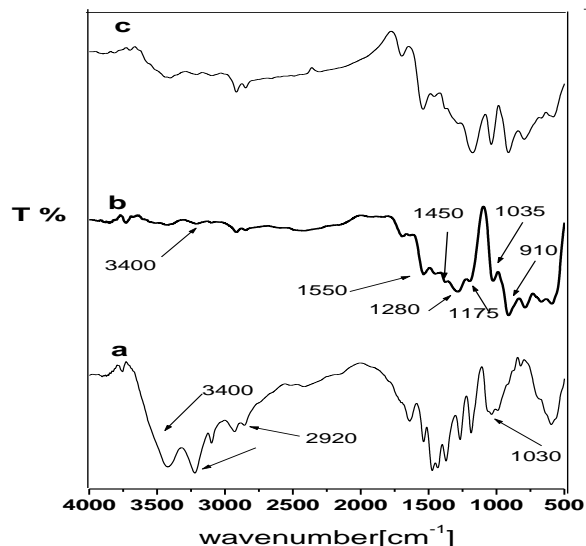


Figure 1: FT-IR spectra of; (a) NC, (b) NPPy/AgNPs, and (c) NC/NPPyAg nanocomposite

3.2 UV-Vis Spectra

The UV-Vis spectrum of the NC/NPPyAg nanocomposite is shown in Fig. 2. The p-p* transition band of PPy appears in the region of 400-500 nm [22], and the plasmonic response of the AgNPs appears at approximately 400 nm, depending on the dielectric constant of the surrounding medium [23]. Therefore, the absorption peak in the NC/NPPy-AgNP nanocomposite results from two contributions: NPPy and the surface absorption of the AgNPs. The absence of the strong absorption from metallic silver at approximately 400 nm for the NC/NPPy-AgNP nanocomposite reveals that the AgNPs are dispersed as nanoparticles within the NC/NPPy-AgNP nanocomposite. In the NC/NPPy-AgNP nanocomposite, the absorption band at 900 nm may be attributed to the in-plane resonance of the AgNPs [24-25]. The absorption band in the NIR region in the composite may indicate the presence of additional channels at the interface of the NPPy-AgNPs to promote electrons from the valance band to the conduction band, leading to a decreased energy required for electronic transitions [26].

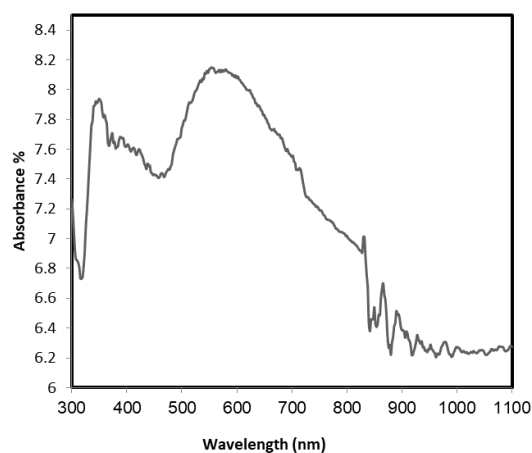


Figure 2: UV-Vis spectra of the NC/NPPy-AgNP composite

3.3 XRD Analysis

Fig. 3 shows the XRD pattern of NC/NPPy-AgNP nanocomposite, displaying four distinct diffraction peaks at 38° , 44° , 64.6° and 78° , which correspond to the (111), (200), (220) and (311) planes, respectively, of the cubic crystalline structure of silver [27]. A broad characteristic peak in the region of 20° to 24° is attributed to the amorphous structure of NPPy, while the peaks at $9^\circ \leq 2\theta \leq 22^\circ$ correspond to the crystalline structure of cellulose [28].

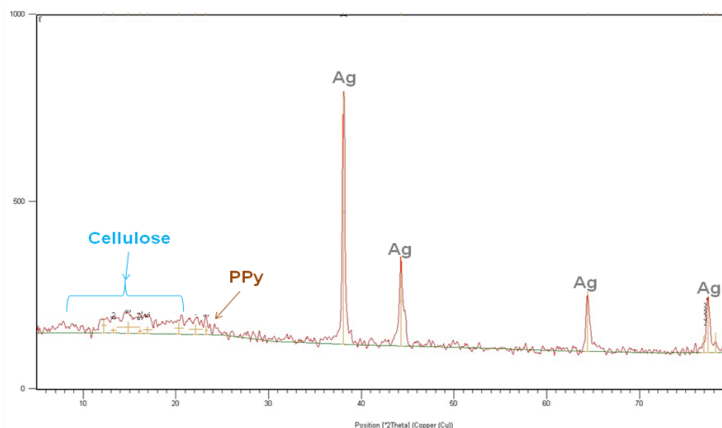


Figure 3: XRD pattern of NC/NPPy-AgNP nanocomposite

3.4 Thermogravimetric Analysis (TGA)

The thermal stabilities of NPPy and the NC/NPPy-AgNP nanocomposite were investigated by TGA, and the curves are shown in Fig. 4. The initial weight loss below 120°C was mainly due to the evaporation of adsorbed water. The weight loss starting from $\sim 150^\circ\text{C}$ was caused by the degradation of the PPy chains. The thermal stability of the NC/NPPy-AgNPs nanocomposite withstood degradation at high temperature.

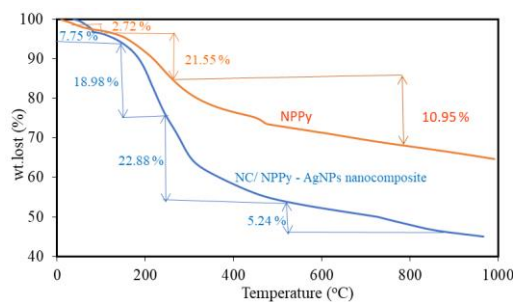


Figure 4: TGA of NPPy, and NC/NPPy-AgNPs nanocomposite

3.5 Transmission Electron Microscopy (TEM)

To investigate the nanostructure of silver, cellulose and PPy, TEM images of the NC/AgNP and NPPy/AgNP composites are given in Fig. 5(A & B). This figure reveals that silver is present in the NC/AgNP and NPPy/AgNP composites as nanoparticles with sizes less than 10 nanometers. The diameter of NC is between 1.2 and 2.13 nanometers. The size of NPPy is between 30 and 70 nanometers.

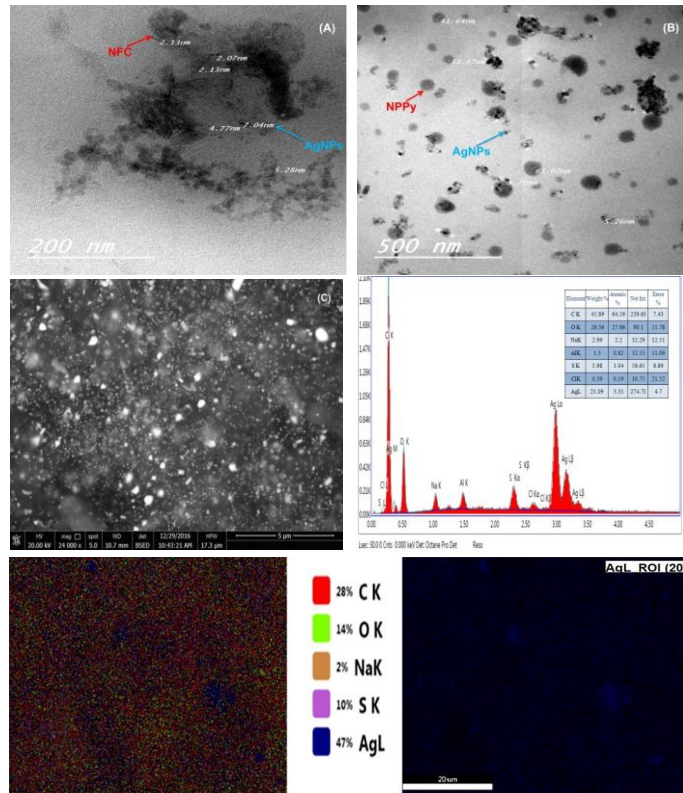


Figure 5: TEM images of the (A) NC/AgNPs, (B) NPPy/AgNPs, and (C) EDX analysis of AgNPs loaded into NC/NPPy-AgNPs nanocomposite

3.6 EDX Analysis

Fig. 5(C) demonstrates the dispersion of the AgNPs in the prepared NC/NPPy-AgNP nanocomposite. EDX analysis evidenced the presence of AgNPs in the composite of NC with NPPy. However, upon polymerization, not only nanosized but also a small number of submicron/micron-sized Ag particles are formed, resulting in the presence of micron-sized Ag aggregates in the matrix. To further analyze the Ag distribution, elemental mapping of Ag is provided in Fig. 5. The homogeneous brightness and distribution proved the even distribution of Ag, which can enhance the dielectric properties of the composite material.

3.7 Dielectric Measurements

To study the effect of the AgNPs on the conductivity of the prepared composite, the amounts of precursors used in the preparation are listed in Tab. 1.

Fig. 6 shows the effect of the additives, i.e., NPPy and AgNPs, on the electrical properties of NC. As seen in Fig. 6(A), the dielectric constants of the prepared samples show a relaxation behavior that can be attributed to different relaxation processes inside the materials, such as interfacial polarization and dipolar polarization. The relaxation behavior [29] appears due to the decreasing speed of the alternating dipoles with an increasing field frequency, before reaching a frequency that does not follow the alternating field. This behavior has a good impact on the electrical properties of the different materials. Fig. 6(A) shows that the dielectric constants of the samples decrease to low values at high frequency. Since the samples under study are composed of electrical heterogeneous phases, i.e., the NC polymer, NPPy conducting polymer and AgNPs, interfacial polarization is the dominant effect on the dielectric constant at low frequency. In heterogeneous composites, charges accumulate at the interfaces between the different phases and hence produce interfacial dipoles that appear in the low-frequency range. Additionally, the high dielectric constants and dielectric losses at low frequency can be attributed to the DC conductivity

contribution to the relaxation processes, since the prepared samples contain the NPPy conducting polymer and AgNPs [30-32]. At high frequency, the dielectric constants and dielectric losses have very small values due to the disappearance of interfacial polarization and orientational polarization, and the only contribution at high frequency may be atomic and electronic polarization.

Fig. 6(A & B) shows that the dielectric constant ϵ' and dielectric loss ϵ'' increased by adding NPPy/AgNPs to the samples. The increasing content may have increased the interfacial polarization due to the blending of the two polymers, NC and NPPy, resulting in trapping of the AgNPs and virtual charge at the polymer interface, which leads to an increase in the total dipole moment in the composite sample.

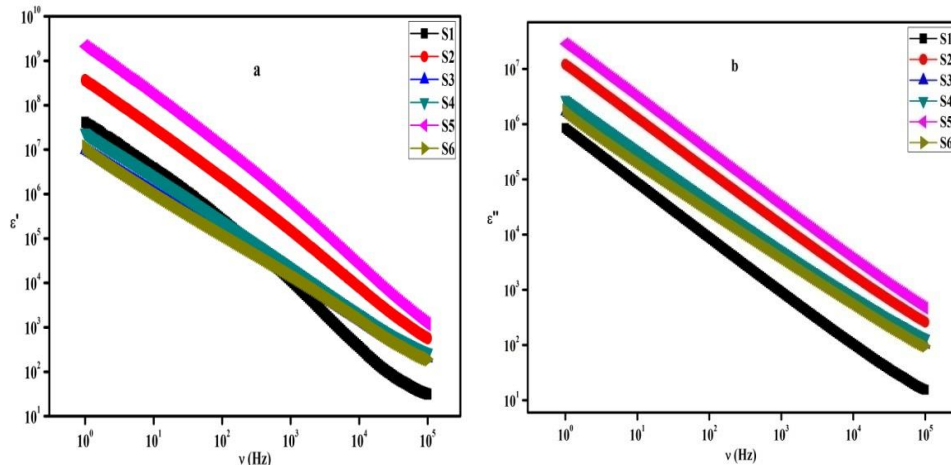


Figure 6: Dielectric constant ϵ' (a) and dielectric loss ϵ'' (b) of NC/NPPy/AgNPs

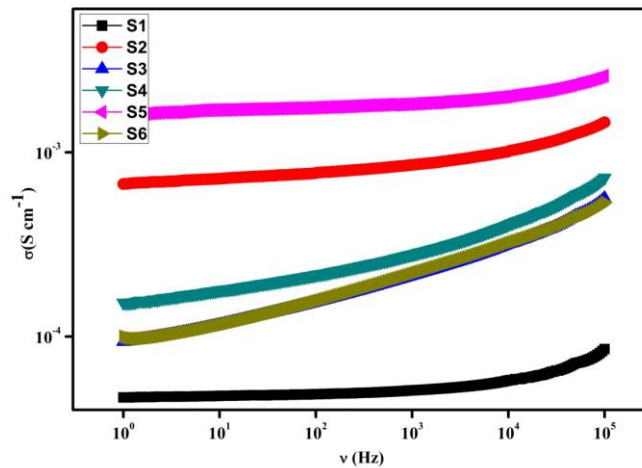


Figure 7: The frequency dependence of AC conductivity

3.8 AC Conductivity

Materials have two conductivity (σ_T) components: direct (σ_{DC}) and alternating conductivity (σ_{AC}). The total conductivity (σ_T) is given by

$$\sigma_T = \sigma_{DC} + \sigma_{ac}(\omega)$$

The first term describes the frequency independent conductivity and can be attributed to band conduction. The second term describes the alternating conductivity, which results from charge-carrier hopping processes and is given by:

$$\sigma_{ac}(\omega) = \varepsilon_0 \varepsilon'' \omega$$

The experimental conductivity $\sigma(\nu)$ of the composites in the frequency range of 1 Hz-100 kHz was calculated from the AC conductance $G(\nu)$ measurements using the following equation:

$$\sigma(\nu) = G(\nu) \cdot \frac{t}{A}$$

where A is the electrode cross-sectional area, and t is the thickness of the sample.

Fig. 7 shows the frequency dependence of the AC conductivity. The experimental conductivity shows two trends in the frequency range from 1 Hz to 100 kHz that can be attributed to DC and AC conductivities. The DC conductivity appears in the low-frequency range from 1 to 10^3 Hz, where the total conductivity is nearly frequency independent in this frequency range and can be attributed to the migration of free charge carriers through the conduction band. The AC conductivity appears in the frequency range from 1 kHz to 100 kHz, where the experimental conductivity shows a frequency dependent response in this frequency range. The AC conductivity in polymeric systems results from hopping processes through defect sites along the polymer chains.

Fig. 7 shows that the conductivity increases with an increasing NPPy content in the sample. The increasing NPPy content in the composite leads to an increased number of sites to facilitate charge-carrier hopping processes. Additionally, increasing the AgNP content improves the charge-carrier density in the composite. Therefore, increasing the NPPy and AgNPs contents in the sample leads to an increase in the total conductivity of the sample, as seen in Fig. 7 [32]. Table 1 indicates that S5 has the highest AC conductivity among the samples.

The present work proves that NPPy and Ag NPs improve the electrical conductivity of the insulator NC. NPPy particles were encapsulated by insulator NC creating a non-conductive shell that leads to decreasing the DC conductivity of NPPy in comparison with Sasso et al results that used small amounts of insulator cellulose as a binder for PPy and obtained high DC conductivity [33,34].

Table 2: AC conductivities of the prepared samples at different frequencies

Frequency	S1 ($\sigma(\text{S cm}^{-1})$)	S2 ($\sigma(\text{S cm}^{-1})$)	S3 ($\sigma(\text{S cm}^{-1})$)	S4 ($\sigma(\text{S cm}^{-1})$)	S5 ($\sigma(\text{S cm}^{-1})$)	S6 ($\sigma(\text{S cm}^{-1})$)
100	4.87338E-5	7.74481E-4	1.54422E-4	2.1593E-4	0.00175	1.56054E-4
1000	5.10558E-5	8.55844E-4	2.15721E-4	2.79236E-4	0.00183	2.20782E-4
10000	5.8087E-5	0.00102	3.20071E-4	4.09215E-4	0.00202	3.24067E-4
50000	7.16597E-5	0.00126	4.52656E-4	5.8665E-4	0.00234	4.42006E-4
100000	8.55766E-5	0.00146	5.63688E-4	7.26896E-4	0.0026	5.34323E-4

4 Conclusions

A NPPy/AgNP composite was chemically synthesized via emulsion polymerization of Py using AgNO_3 as an oxidizing agent in the presence of a surfactant dopant. PPy nanoparticles with sizes of 30-70 nm with specific conductivity in the range of 10^{-5} S/cm were achieved.

Additionally, polymeric conducting nanocomposites containing AgNPs were prepared with important polymers, such as NC and NPPy. The AgNPs acted as an oxidizing agent to incorporate nanoparticles in the prepared composite. From scanning electron microscopy (SEM) measurements, a

homogeneous distribution of AgNPs was observed. An optimum conductivity of 10^{-3} S/cm was achieved with prepared nanocomposite prepared from 2 g of NC, 16.7 ml of Py and 4.3 g of AgNO_3 .

Conflicts of Interest: The authors declare no conflicts of interest.

Acknowledgement: The authors acknowledge the Science and Technology Development Fund (STDF), Egypt and Scientific Research Support Fund (SRSF), Jordan for financial support of the research activities related to this project; Project ID 22929.

References

1. Jangid NK, N. Chauhan PS, Meghwal K, Ameta R, Punjabi P B. A review: conducting polymers and their applications. *Research Journal of Pharmaceutical, Biological and Chemical Sciences* **2014**, 5(3): 383-412.
2. Pecher J, Mecking S. Nanoparticles of conjugated polymers. *Chemical Reviews* **2010**, 110(10): 6260-6279.
3. Shi ZQ, Zhou H, Qing XT, Tingyang Dai TY, Lu Y. Facile fabrication and characterization of poly(tetrafluoroethylene) @polypyrrole/nano-silver composite membranes with conducting and antibacterial property. *Applied Surface Science* **2012**, 258: 6359-6365.
4. Varesano A, Vineis C, Aluigi A, Rombaldoni F, Tonetti C, Mazzuchetti G. Water-insoluble keratin nanofibres by electrospinning from water solutions. *Synthetic Metals* **2006**, 156(5-6): 379-386.
5. Johnston JH, Moraes J, Borrmann T. Conducting polymers on paper fibres. *Synthetic Metals* **2005**, 153: 65-68.
6. AL-Oqla FM, Sapuan SM, Anwer T, Jawaid M, Hoque ME.: Dynamic mechanical properties of fibre reinforced polymer composites: a review. *Synthetic Metals* **2015**, 206: 42-54.
7. AmanyM E, AhmedAH, Imad H, kamel S. Conducting cellulose-nano composites by in situ polymerization of pyrrole. *Carbohydrate Polymers* **2017**, 168: 182-190.
8. Madaeni SS. Preparation and properties of composite membranes composed of non-conductive membranes and polypyrrole. *Indian Journal of Chemical Technology* **2006**, 13: 65-70.
9. Ahmed K, Shaikh F, Shaheer MM, Moku B, Shaik B, Rafique HS. Convenient synthesis of substituted pyrroles via a cerium (IV) ammonium nitrate (CAN)-catalyzed Paal-Knorr reaction. *Arabian Journal of Chemistry* **2016**, 9(4): 542-549.
10. Hemant KC, Narendra VB, Vasant EW, Ganesh NS. Synthesis of polypyrrole using ferric chloride (FeCl_3) as oxidant together with some dopants for use in gas sensors. *Journal of Sensor Technology* **2011**, 1: 47-56.
11. Molina J, del Río AI, Bonastre J, Cases F. Electrochemical polymerisation of aniline on conducting textiles of polyestercovered with polypyrrole/AQSA. *European Polymer Journal* **2009**, 45(4): 1302-1315.
12. Zhang D, Zhang Q, Gao X, Piao G. A nanocellulose polypyrrole composite based on tunicate cellulose. *International Journal of Polymer Science* **2013**, 2013:1-6.
13. Kim SY, Hong J, Tayhas G, Palmore R. Polypyrrole decorated cellulose for energy storage applications. *Synthetic Metals* **2012**, 162:1478-1481.
14. Bober P, Liu J, Mikkonen KS, Ihalainen P, Pesonen M et al. Biocomposites of nanofibrillated cellulose, polypyrrole, and silver nanoparticles with electroconductive and antimicrobial properties. *Biomacromolecules* **2014**, 15(10): 3655-3663.
15. Chen F, Liu P. Conducting polyaniline nanoparticles and their dispersion for waterborne corrosion protection coatings. *ACS Applied Material Interfaces* **2011**, 3: 2694-2702.
16. Jing S, Xing S, Yu L, Zhao C. Synthesis and characterization of Ag/polypyrrole nanocomposites based on silver nanoparticles colloid. *Material Letters* **2007**, 61: 4528-4530.
17. Babu KF, Dhandapani P, Maruthamuthu S, Kulandainathan MA. One pot synthesis of polypyrrole silver nanocomposite on cotton fabrics for multifunctional property. *Carbohydrate Polymer* **2012**, 90: 1557-1563.

18. Anuj K, Yuvraj SN, Veena C, Nishi KB. Characterization of Cellulose Nanocrystals Produced by Acid-Hydrolysis from Sugarcane Bagasse as Agro-Waste. *Journal of Materials Physics and Chemistry* **2014**, 2(1): 1-8.
19. Ortiz-Serna P, Díaz-Calleja R, Sanchis MJ, Riande E, Nunes R et al. Dielectric spectroscopy of natural rubber-cellulose II nanocomposites. *Journal of Non-Crystalline Solids* **2011**, 357: 598-604.
20. Silva CC, Valente MA, Graça MPF, Góes JC, Sombra ASB. Microwave preparation, structure and electrical properties of calcium-sodium-phosphate biosystem. *Journal of Non-Crystalline Solids* **2006**, 352(32-35): 3512-3517.
21. Muller D, Rambo CR, Recouvreux C R, Porto LM, Barra GMO. Chemical in situ polymerization of polypyrrole on bacterial cellulose nanofibers. *Synthetic Metals* **2011**, 161(1-2): 106-111.
22. Liu YC, Chuang TC. Synthesis and characterization of gold/polypyrrole core-shell nanocomposites and elemental gold nanoparticles based on the gold-containing nanocomplexes prepared by electrochemical methods in aqueous solutions. *The Journal of Physical Chemistry B* **2003**, 107(45): 12383-12386.
23. Ullah MH, Kim I, Ha CS. In-situ preparation of binary-phase silver nanoparticles at a high Ag concentration. *Journal of Nanoscience Nanotechnology* **2006**, 6(3): 777-782.
24. Ullah MH, Ha CS. In situ prepared polypyrrole-Ag nanocomposites: optical properties and morphology. *Journal of Materials Science* **2016**, 51(16): 7536-7544.
25. Chen A, Kamata K, Nakagawa M, Iyoda T, Wang H, Li X. Formation process of silver-polypyrrole coaxial nanocables synthesized by redox reaction between AgNO₃ and pyrrole in the presence of poly(vinylpyrrolidone). *Journal of Physical Chemistry B* **2005**, 109(39): 18283-18288.
26. Chitte HK, Bhat NV, Karmakar NS, Kothari DC, Shinde GN. Synthesis and characterization of polymeric composites embedded with silver nanoparticles. *World Journal of Nano Science and Engineering* **2012**, 2: 19-24.
27. Song P, Wang Q, Yang ZX. Ammonia Gas Sensor Based on PPy/ZnSnO₃ Nanocomposites. *Materials Letters* **2011**, 65(3): 430-432.
28. Ericka N, Johnson F, Sharathkumar KM, Shelby FT, James WR. X-ray diffraction of cotton treated with neutralized vegetable oil-based macromolecular crosslinkers. *Journal of Engineered Fibers and Fabrics* **2010**, 5(1): 10-20.
29. Vijayalakshmi R, Ashokan PV, Shridhar MH. Studies of dielectric relaxation and a.c. conductivity in cellulose acetate hydrogen phthalate-poly(methyl methacrylate) blends. *Materials Science and Engineering A* **2000**, 281: 213-220.
30. Nada AMA, Dawy M, Salama AH. Dielectric properties and ac-conductivity of cellulose polyethylene glycol blends. *Materials Chemistry and Physics* **2004**, 84: 205-215.
31. El-Sayed S, Mahmoud KH, Fatah AA, Hassen A. DSC, TGA and dielectric properties of carboxymethyl cellulose/polyvinyl alcohol blends. *Physica. B* **2011**, 406: 4068-4076.
32. Kumar A, Sarmah S. AC conductivity and dielectric spectroscopic studies of polypyrrole-titanium dioxide hybrid nanocomposites. *Physics Status Solidi, A* **2011**, 208(9): 2203-2210.
33. Sasso C, Zeno E, Petit-Conil M, Chaussy D, Belgacem MN, Tapin-Lingua S, Beneventi D. Highly conducting polypyrrole/cellulose nanocomposite films with enhanced mechanical properties. *Macromolecular Material and Engineering* **2010**, 295: 934-941.
34. Sasso C, Bruyant N, Beneventi D. Polypyrrole (PPy) chemical synthesis with xylan in aqueous medium and production of highly conducting PPy/nanofibrillated cellulose films and coatings. *Cellulose* **2011**, 18: 1455-1461.